A Study of Thermally Radiant Williamson Nanofluid Over an Exponentially Elongating Sheet with Chemical Reaction Via Homotopy Analysis Method

Cheela Sunitha[1], Prathi Vijaya Kumar[1,*], Giulio Lorenzini[2], Shaik Mohammed Ibrahim[3]

[1] Department of Mathematics, GITAM (Deemed to be University), Visakhapatnam, Andhra Pradesh 530045, India
[2] Department of Engineering and Architecture, University of Parma, Parco Area delle Scienze 181/A, Parma 43124, Italy
[3] Department of Mathematics, Koneru Lakshmaiah Education Foundation, Vaddeswaram, Guntur, Andhra Pradesh, - 522302, India

ARTICLE INFO	ABSTRACT
	This paper explores the role of thermal radiation, viscous dissipation and chemical reaction on stagnation point flow of Williamson nanofluid over an exponentially stretching sheet. The similarity transformations are performed to extract ordinary differential equations (ODEs) via partial differential equations (PDEs) and the simulation was accomplished by employing homotopy analysis method (HAM). In addition, we evaluated by comparing our findings to those previously described for specific occurrences which are in perfect unison. Skin friction, Nusselt number and Sherwood numbers are captured in the form of graphs and tables for distinct quantities of the flow parameters. The skin friction coefficient improves as the Williamson fluid parameter is elevated.

1. Introduction

Nanofluids are nanometer-sized particles less than 100 nanometres in size that are introduced into base fluids such as oil, water, bio fluids, ethylene, and lubricants. Despite their essential worth in industry, medicine, and a variety of other efficacious domains of science and technology, countless researchers have gained an interest in nanofluids as opposed to other fluids. However, nanofluids still occupy an indispensable key position in medical sectors, such as the use of gold nanoparticles in the screening of cancerous tumours and the processing of minuscule bombs that are exploited to eradicate cancerous tumours. Choi and Eastman [1] was the one who came up with the idea of nano materials. He inferred from his observations that infusing these particles strengthens the thermal conductivity of the fluid. Hayat *et al.,* [2] produced analytical solutions for MHD nanofluid squeezing flow between two parallel plates. Makinde and Aziz [3] looked how an electrically conducting nanofluid distributes heat and mass over a radially stretched surface in the context of thermophoresis and Brownian motion. The consequence of escalating nonlinear thermal radiation on boundary layer flow of several nanofluids is explored by Mahanthesh *et al.,* [4]. The strengthening

---

of the heat transmission rate with regular carrier liquids is highlighted in distinct scholarly articles pertaining to nano liquids [5-11].

Many published studies have evaluated MHD flow behaviour due to the multitude application scenarios of MHD in technological processes. Some occurrences of certain domains include fusing metals in an induction furnace generating a magnetic field and cooling the first layer around a nuclear reactor containment dome utilising a magnetic field to segregate the hot plasma from the wall. The external magnetic field might still perform an indispensable key position in influencing momentum and heat transfers in the boundary layer flow of multiple fluids together across stretching sheet. This has been undertaken in geophysical and astrophysical science to perceive and acknowledge about solar structures, radio propagation across the ionosphere, and so forth. Emancipated convective fluxes are significant in engineering and industrial sectors such as geothermal structures, fibre and granular insulations, and so on. Khan *et al.,* [12] discussed the rapidly moving stretched surface subjected to MHD boundary layer nanofluid flow. Daniel *et al.,* [13] employed variable thickness and thermal radiation to assess an MHD nanofluid over a nonlinear stretching sheet. Mustafa and Khan [14] analyzed the performance of a magnetic field on Casson nanofluid when that was stretched nonlinearly.

Stagnation-point flow occurs when a fluid impinges on a solid object in any sort of flow. At the stagnation point, the fluid velocity drops to zero, and the fluid pressure and heat mass transfer rates are at their maximum. The stagnation point flow across a permeable shrinking sheet was addressed by Bhatti *et al.,* [15]. Mabood *et al.,* [16] explored the role of a chemical reaction on MHD stagnation point flow near a stretching sheet with injection/suction. The tabular reactor, oxidations of solid materials, and the synthesis of ceramics materials are all essential equipment in the study of chemically reacting fluid flow. Abbas *et al.,* [17] evaluated the diffusion of chemical reactive species by studying homogeneous–heterogeneous reactions.

It is essential to mention that innumerable non-Newtonian fluids are exploited in industry. Non-Newtonian fluids are now widely acknowledged as contributing in engineering and industrial applications. Pseudoplastic fluids has broad spectrum of applications in petroleum industry and power engineering. Williamson fluid is one such fluid which exhibits the properties of Pseudoplastic fluids. Williamson developed a mathematical model of Pseudoplastic materials in 1929 and provided an equation-based concept to capture the flow of Pseudoplastic fluids, which has already been empirically proven. Malik *et al.,* [18] studied homogeneous-heterogeneous interactions in the Williamson fluid model across a stretching cylinder. Impact of pressure dependent viscosity on Williamson fluid flow has been explored by Zehra *et al.,* [19]. Much insight on this theme can be found in Bakar and Soid [20], Mabood *et al.,* [21], Ibrahim *et al.,* [22], Thirupathi *et al.,* [23], Rosaidi *et al.,* [24], Osman *et al.,* [25], and Japili *et al.,* [26].

Viscos dissipation is a concept adopted in fluid mechanics to characterize the extinction of oscillating velocity gradients driven by viscous stresses. The transition of kinetic energy into internal energy of the fluid is a phrase used to refer this partially irreversible phenomenon. Engineers and scientists are also fascinated in energy dissipation and non-Newtonian fluid flow. Acknowledging energy dissipation and transport in nanoscale structures, according to Pop [27], is crucial for the design of energy-efficient circuits and energy-conversion devices. Engineers and scientists are also fascinated in energy dissipation and non-Newtonian fluid flow. Ajayi *et al.,* [28] discussed viscous dissipation implications in a non-Newtonian Casson fluid flow across a paraboloid of revolution's upper horizontal thermally stratified melting surface. Khan *et al.,* [29] looked into how partial slip influenced Williamson stagnation nanofluid flow over a stretching/shrinking surface. In the fluid flow phenomenon, the outcomes of thermal radiation and heat transfer are crucial. Owing of its prominence, multiple researchers have explored the role of thermal radiation, thermal slip, and heat

transfer on MHD stagnation-point flow for distinct geometrical scenarios. The stagnation point flow of a magnetised Williamson fluid via a stretched sheet is addressed in the vicinity of nonlinear thermal radiation and the buoyancy factor by Rajput *et al.,* [30].

This research emphasizes on the heat and mass transfer analysis of Williamson nanofluid where the sheet stretches exponentially using HAM, which has been formerly overlooked [31-35].

2. Mathematical Formulation

Consider a steady, two-dimensional Williamson nanofluid stagnation point flow across an exponentially stretching sheet. Here, stretching and free stream velocities are speculated as and respectively, where are constants, is the coordinate measure along the stretching surface and is the length of the sheet. A non-uniform transverse magnetic field of strength is introduced parallel to axis, where is the uniform magnetic field strength. The induced magnetic field generated by the movement of an electrically conducting field is presumed to be insignificant. Additionally, the external electric field is presumed to be zero, and the electrical field owing to charge polarization is insignificant. Flow description is given in Figure 1.
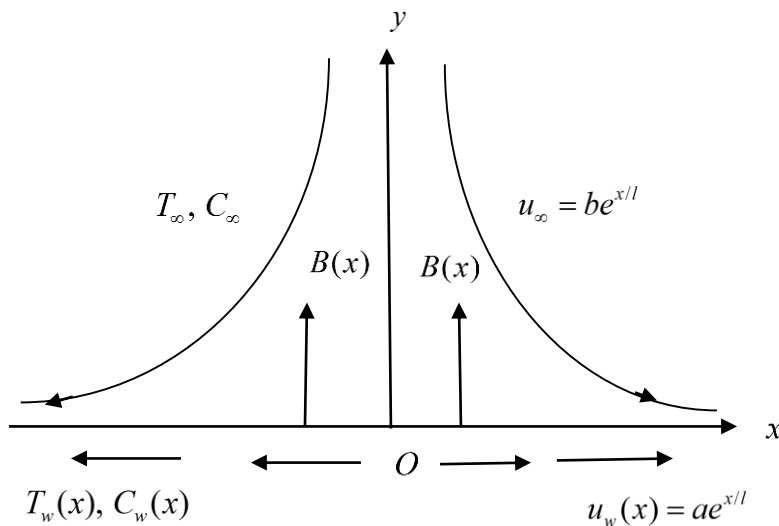

Fig. 1. Physical model of the flow

The governing boundary layer equations based on the stated constraints are [33]:

$$\frac{\partial u}{\partial x} + \frac{\partial v}{\partial y} = 0,$$ (1)

$$u\frac{\partial u}{\partial x} + v\frac{\partial u}{\partial y} = \sqrt{2}v\,\Gamma\frac{\partial u}{\partial y}\frac{\partial^2 u}{\partial y^2} + u_\infty\frac{du_\infty}{dx} + v\frac{\partial^2 u}{\partial y^2} + \frac{\sigma B^2(x)}{\rho_f}[u_\infty - u],$$ (2)

$$u\frac{\partial T}{\partial x} + v\frac{\partial T}{\partial y} = \alpha\frac{\partial^2 T}{\partial y^2} - \frac{1}{(\rho C_p)_f}\frac{\partial q_r}{\partial y} + \tau\left[D_B\left(\frac{\partial C}{\partial y}\frac{\partial T}{\partial y}\right) + \frac{D_T}{T_\infty}\left(\frac{\partial T}{\partial y}\right)^2\right] + \frac{\mu}{(\rho C_p)_f}\left(\frac{\partial u}{\partial y}\right)^2,$$ (3)

$$u\frac{\partial C}{\partial x}+v\frac{\partial C}{\partial y}=D_B\left(\frac{\partial^2 C}{\partial y^2}\right)+\frac{D_T}{T_\infty}\left(\frac{\partial^2 T}{\partial y^2}\right)-Kr\left(C-C_\infty\right).\tag{4}$$

Subject to the boundary conditions

$$\begin{aligned}
&u=u_w(x)=ae^{x/l},\ \ v=0,\ T=T_W(x),\ C=C_w(x)\quad at\quad y=0\\
&u\rightarrow u_\infty(x)=be^{x/l},\ \ v\rightarrow 0,\ T\rightarrow T_\infty,\ C\rightarrow C_\infty\quad as\quad y\rightarrow\infty
\end{aligned}\tag{5}$$

The prescribed temperature and concentration on the surface of the sheet is assumed to be $T_w(x)=T_\infty+T_0e^{x/2l}$ and $C_w(x)=C_\infty+C_0e^{x/2l}$ where T_0,C_0 are the reference temperature and concentration respectively, now, the stream function $\psi=\psi(x,y)$ is characterized as

$$u=\frac{\partial\psi}{\partial y},v=-\frac{\partial\psi}{\partial x},$$

where Eq. (1) is satisfied identically.

Here, u and v are the velocity components in x and y directions, $v=\dfrac{\mu}{\rho}$ is the kinematic viscosity, ρ is the fluid density, σ is the electrical conductivity of the fluid, μ is the coefficient of viscosity, C_p is the specific heat at constant pressure, k is the thermal conductivity, q_r is the radiative heat flux, T and C are the fluid temperature and nanoparticle concentration, T_w and C_w are the wall surface temperature and nanoparticle concentration, T_∞ and C_∞ are the fluid temperature and nanoparticle concentration far from the sheet, , Γ is the time constant, $\alpha=\dfrac{k}{\left(\rho C_p\right)_f}$ is the thermal diffusivity, $\tau=\dfrac{\left(\rho C_p\right)_p}{\left(\rho C_p\right)_f}$ is the fraction of heat capability of nanofluid to the base fluid, D_B is the Brownian motion constant, D_T is the thermophoresis diffusion and Kr is the chemical reaction parameter.

Following Rosseland approximation, the radiative heat flux is

$$q_r=-\frac{4\sigma^*}{3k^*}\frac{\partial T^4}{\partial y},$$

where σ^* is the Stefan-Boltzman constant and k^* is the mean absorption coefficient. We also suppose that the temperature difference within the flow is large enough that T^4 is expressed as a linear function of temperature. As a result, by expanding T^4 in Taylor series about T_∞ while ignoring higher order terms, we get

$$\mathrm{T}^4\cong 4T_\infty^3 T-3T_\infty^4.$$

The succeeding similarity transformations are now initiated:

$$\psi = \sqrt{2lva}\, e^{x/2l} f(\zeta), \theta(\zeta) = \frac{T - T_\infty}{T_w - T_\infty}, \phi(\zeta) = \frac{C - C_\infty}{C_W - C_\infty}, \zeta = y\sqrt{a/2vl}\, e^{x/2l}. \tag{6}$$

Now Eq. (2) to Eq. (5) become

$$f''' + \lambda f'' f''' + ff'' - 2f'^2 + 2\varepsilon^2 + M(\varepsilon - f') = 0, \tag{7}$$

$$\frac{1}{\Pr}\left(1 + \frac{4R}{3}\right)\theta'' + f\theta' - f'\theta + Nb\,\phi'\,\theta' + Nt\,\theta'^2 + Ec\,f'^2 = 0, \tag{8}$$

$$\phi'' + Le\,f\phi' - Le\,f'\phi + \frac{Nt}{Nb}\theta'' - \gamma\,Le\,\phi = 0. \tag{9}$$

The boundary conditions are

$$\begin{aligned} &f(\zeta) = 0, f'(\zeta) = 1, \theta(\zeta) = 1, \phi(\zeta) = 1 \quad at \quad \zeta = 0, \\ &f'(\zeta) \to \varepsilon, \theta(\zeta) \to 0, \phi(\zeta) \to 0 \qquad as \quad \zeta \to \infty. \end{aligned} \tag{10}$$

Where $\varepsilon = b/a$ is the velocity ratio parameter, $\lambda = \Gamma\sqrt{\dfrac{a^3 e^{\frac{3x}{l}}}{vl}}$ is the Williamson parameter, $M = \dfrac{2l\sigma B_0^2}{a\rho_f}$ is the magnetic parameter, $R = \dfrac{4\sigma^* T_\infty^3}{k^* k}$ is the radiation parameter, $\Pr = \dfrac{v}{\alpha}$ is the Prandtl number, $Nb = \dfrac{\tau D_B(C_w - C_\infty)}{v}$ is the Brownian motion parameter, $Nt = \dfrac{\tau D_T(T_w - T_\infty)}{T_\infty v}$ is the thermophoresis parameter, $Ec = \dfrac{u_w^2}{(C_p)_f(T_w - T_\infty)}$ is the Eckert number, , $Le = \dfrac{v}{D_B}$ is the Lewis number, $\gamma = \dfrac{2l\,Kr}{u_w}$ is the chemical reaction parameter.

Non-dimensional skin friction coefficient C_f, Nusselt number Nu_x and Sherwood number are

$$C_f = \frac{\tau_w}{\rho u_w^2},, \quad \text{where} \quad \tau_w = \mu\frac{\partial u}{\partial y}\left(1 + \frac{\Gamma}{\sqrt{2}}\left(\frac{\partial u}{\partial y}\right)^2\right)_{y=0}, \quad Nu_x = \frac{xq_w}{k(T_w - T_\infty)} \text{ and the Sherwood number}$$

$$Sh_x = \frac{xq_m}{D_B(C_w - C_\infty)},$$

where q_w and q_m are the heat flux and mass flux at the surface respectively given by

$$q_w = \left(-\left(k + \frac{16\sigma^* T_\infty^3}{3k^*}\right)\left(\frac{\partial T}{\partial y}\right)\right)_{y=0}, \quad q_m = -\left(D_B\left(\frac{\partial u}{\partial y}\right)\right)_{y=0}$$

Substituting q_w and q_m in the preceding equation, we get

$$\sqrt{2}\,\mathrm{Re}_x^{1/2}\,C_f = \left(f''(0) + \frac{\lambda}{2}(f''(0))^2\right), \quad \sqrt{2}\,\mathrm{Re}_x^{1/2}\,Nu_x = -\left(1 + \frac{4R}{3}\right)\theta'(0) \text{ and}$$

$$\sqrt{2}\,\mathrm{Re}_x^{1/2}\,Sh_x = -\phi'(0),$$

where $\mathrm{Re}_x = \dfrac{u_w x}{\nu}$ is the local Reynolds number.

2.1 HAM

We use the mentioned initial guesses and linear operators to encapsulate the homotopic approaches of Eq. (7) to Eq. (10).

$$f_0(\zeta) = \zeta\varepsilon + (1-\varepsilon)(1-e^{-\zeta}),$$
$$\theta_0(\zeta) = e^{-\zeta},$$
$$\phi_0(\zeta) = e^{-\zeta},$$

$$L_1(f) = f''' - f',$$
$$L_2(\theta) = \theta'' - \theta,$$
$$L_3(\phi) = \phi'' - \phi,$$

with

$$L_1\left(C_1 + C_2 e^{\zeta} + C_3 e^{-\zeta}\right) = 0,$$
$$L_2\left(C_4 e^{\zeta} + C_5 e^{-\zeta}\right) = 0,$$
$$L_3\left(C_6 e^{\zeta} + C_7 e^{-\zeta}\right) = 0,$$

where C_i ($i = 1$ to 7) are the arbitrary constants.

We construct the zeroth-order deformation equations

$$(1-p)L_1\big(f(\zeta;p) - f_0(\zeta)\big) = p\hbar_1\, N_1[f(\zeta;p)], \tag{11}$$

$$(1-p)L_2\big(\theta(\zeta;p) - \theta_0(\zeta)\big) = p\hbar_2\, N_2[f(\zeta;p), \theta(\zeta;p), \phi(\zeta;p)], \tag{12}$$

$$(1-p)L_3\big(\phi(\zeta;p) - \phi_0(\zeta)\big) = p\hbar_3\, N_3[f(\zeta;p), \theta(\zeta;p), \phi(\zeta;p)], \tag{13}$$

subject to the boundary conditions

$$
\begin{aligned}
f(0;p)&=0, & f'(0;p)&=1, & f'(\infty;p)&=\varepsilon, \\
\theta(0;p)&=1, & & & \theta(\infty;p)&=0, \\
\phi(0;p)&=1, & & & \phi(\infty;p)&=0,
\end{aligned}
\tag{14}
$$

where

$$
\begin{aligned}
N_1\big[f(\zeta;p)\big] &= \frac{\partial^3 f(\zeta;p)}{\partial \zeta^3} + \lambda\,\frac{\partial^2 f(\zeta;p)}{\partial \zeta^2}\frac{\partial^3 f(\zeta;p)}{\partial \zeta^3} + f(\zeta;p)\frac{\partial^2 f(\zeta;p)}{\partial \zeta^2} \\
&\quad -2\left(\frac{\partial f(\zeta;p)}{\partial \zeta}\right)^2 + 2\varepsilon^2 + M\left(\varepsilon - \frac{\partial f(\zeta;p)}{\partial \zeta}\right),
\end{aligned}
\tag{15}
$$

$$
\begin{aligned}
N_2\big[f(\zeta;p),\theta(\zeta;p),\phi(\zeta;p)\big] &= \frac{1}{\Pr}\left(1+\frac{4}{3}R\right)\frac{\partial^2 \theta(\zeta;p)}{\partial \zeta^2} \\
&\quad +\left(f(\zeta;p)\frac{\partial \theta(\zeta;p)}{\partial \zeta} - \theta(\zeta;p)\frac{\partial f(\zeta;p)}{\partial \zeta}\right) + Nb\,\frac{\partial \theta(\zeta;p)}{\partial \zeta}\frac{\partial \phi(\zeta;p)}{\partial \zeta} \\
&\quad +Nt\left(\frac{\partial \theta(\zeta;p)}{\partial \zeta}\right)^2 + Ec\left(\frac{\partial f(\zeta;p)}{\partial \zeta}\right)^2,
\end{aligned}
\tag{16}
$$

$$
\begin{aligned}
N_3\big[f(\zeta;p),\theta(\zeta;p),\phi(\zeta;p)\big] &= \frac{\partial^2 \phi(\zeta;p)}{\partial \zeta^2} + Le\,f(\zeta;p)\frac{\partial \phi(\zeta;p)}{\partial \zeta} \\
&\quad -Le\,\theta(\zeta;p)\frac{\partial f(\zeta;p)}{\partial \zeta} + \frac{Nt}{Nb}\frac{\partial^2 \theta(\zeta;p)}{\partial \zeta^2} - Le\,\gamma\phi(\zeta;p),
\end{aligned}
\tag{17}
$$

where $p\in[0,1]$ is the embedding parameter, $\hbar_1,\hbar_2$ and $\hbar_3$ are non-zero auxiliary parameters and N_1,N_2 and N_3 are nonlinear operators.

The nth-order deformation equations are follows

$$
L_1\big(f_n(\zeta) - \chi_n\,f_{n-1}(\zeta)\big) = \hbar_1\,R_n^f(\zeta),
\tag{18}
$$

$$
L_2\big(\theta_n(\zeta) - \chi_n\,\theta_{n-1}(\zeta)\big) = \hbar_2\,R_n^\theta(\zeta),
\tag{19}
$$

$$
L_3\big(\phi_n(\zeta) - \chi_n\,\phi_{n-1}(\zeta)\big) = \hbar_3\,R_n^\phi(\zeta),
\tag{20}
$$

with the following boundary conditions

$$
\begin{aligned}
f_n(0)&=0, & f_n'(0)&=0, & f_n'(\infty)&=0, \\
\theta_n(0)&=0, & & & \theta_n(\infty)&=0, \\
\phi_n(0)&=0, & & & \phi_n(\infty)&=0,
\end{aligned}
\tag{21}
$$

where

$$R_n^f(\zeta) = f_{n-1}''' + \lambda \sum_{i=0}^{n-1} f_{n-1-i}'' f_i'' + \sum_{i=0}^{n-1} f_{n-1-i} f_i'' - 2\sum_{i=0}^{n-1} f_{n-1-i}' f_i' + (1-\chi_n)(\varepsilon^2 + M) - M f_{n-1}', \tag{22}$$

$$R_n^\theta(\zeta) = \frac{1}{\mathrm{Pr}}\left(1 + \frac{4R}{3}\right)\theta_{n-1}'' + \sum_{i=0}^{n-1} f_{n-1-i} \theta_i' - \sum_{i=0}^{n-1} \theta_{n-1-i} f_i' + Nb\sum_{i=0}^{n-1} \theta'_{n-1-i} \phi_i'$$
$$+ Nt\sum_{i=0}^{n-1} \theta'_{n-1-i} \theta_i' + Ec\sum_{i=0}^{n-1} f_{n-1-i} f_i', \tag{23}$$

$$R_n^\phi(\zeta) = \phi_{n-1}'' + Le\left(\sum_{i=0}^{n-1} f_{n-1-i} \phi_i' - \sum_{i=0}^{n-1} \phi_{n-1-i} f_i' - \gamma\phi_{n-1}\right) + \frac{Nt}{Nb}\theta_{n-1}'', \tag{24}$$

$$\chi_n = \begin{cases} 0, & n \le 1, \\ 1, & n > 1. \end{cases}$$

2.2 Convergence of HAM Solution

The auxiliary parameters $\hbar_1, \hbar_2 \& \hbar_3$ are extremely significant for the convergence and interpolation rate of the specific inferences. Thus, $\hbar$-curves are acknowledged in Figure 2 in order to achieve the requisite quantities for the parameters. The principal scenario of the parameters is only about $[-0.86, 0.0]$, which is exploited from such a precise explanation. For $\hbar_1 = \hbar_2 = \hbar_3 = -0.61$, the series solutions are convergent across the whole ζ area. The convergence of the approach is implied by Table 1.
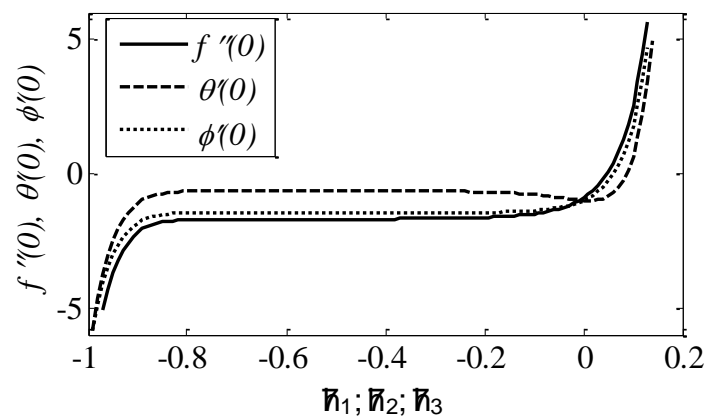

Fig. 2. $\hbar$-curves for $f''(0), \theta'(0)$ and $\phi'(0)$ at 15$^{\text{th}}$ order approximations

Table 1
Convergence of HAM solution for different orders of approximations
when $\lambda = 0.2,\ \varepsilon = 0.1,\ M = 0.5,\ R = 0.1,\ \mathrm{Pr} = 2.0,\ Nb = 0.5,$
$Nt = 0.2,\ Ec = 0.2,\ Le = 2.0,\ \gamma = 0.2.$

Order	$-f''(0)$	$-\theta'(0)$	$-\phi'(0)$
5	-1.253503	0.766873	1.445153
10	-1.253432	0.768051	1.445672
15	-1.253432	0.768047	1.445602
20	-1.253432	0.768046	1.445604
25	-1.253432	0.768046	1.445605
30	-1.253432	0.768046	1.445605
35	-1.253432	0.768046	1.445605
40	-1.253432	0.768046	1.445605

3. Results and Discussion

HAM has been exploited to address the modified equations which have been exposed to boundary conditions. For varying values of the controlling parameters, graphs are plotted for distinct profiles. A comparison with past trends was carried out to ascertain the veracity of our effort, and we got tremendous agreements, as made clear in the Table 2. We include the relevant values during whole evaluation as given below with the exemption of rebuilt values as shown in the tables and graphs.

$\lambda = 0.2,\ \varepsilon = 0.1,\ M = 0.5,\ R = 0.1,\ \mathrm{Pr} = 2.0,\ Nb = 0.5,\ Nt = 0.2,\ Ec = 0.2,\ Le = 2.0,\ \gamma = 0.2.$

It can be evident that as the Williamson fluid parameter λ is grown, $f(\zeta)$ lowers since the fluid produces higher amount of friction, lowering velocity. But with the elevation of λ, the temperature and nanoparticle volume fraction profiles improve. This is given in Figure 3 to Figure 5.
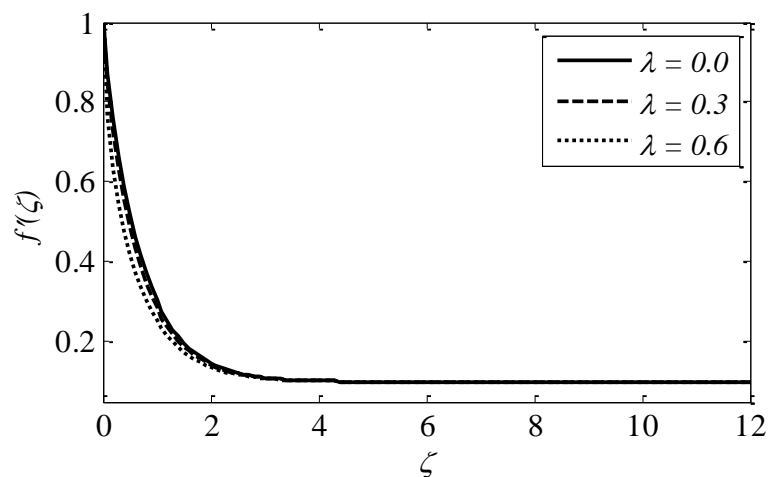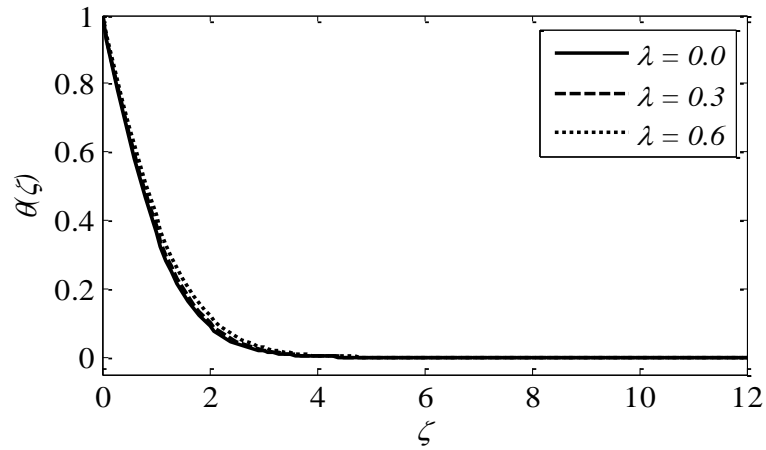

Fig. 3. Profiles of $f'(\zeta)$ for λ

Fig. 4. Profiles of $\theta(\zeta)$ for λ
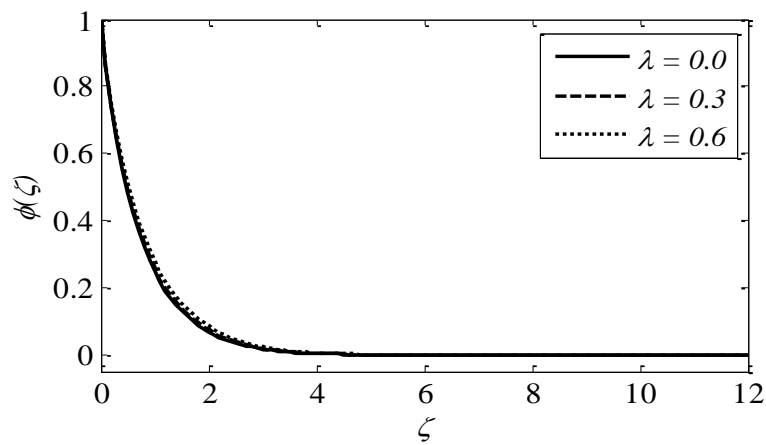

Fig. 5. Profiles of $\phi(\zeta)$ for λ

Figure 6 to Figure 8 reveal the impact of magnetic parameter M on the profiles. $f(\zeta)$ diminishes as the magnitude of M climbs, although the temperature and concentration have the reverse pattern. Actually, the rate of transport falls as M raises because the Lorentz force, which restricts fluid motion, grows as M increases.
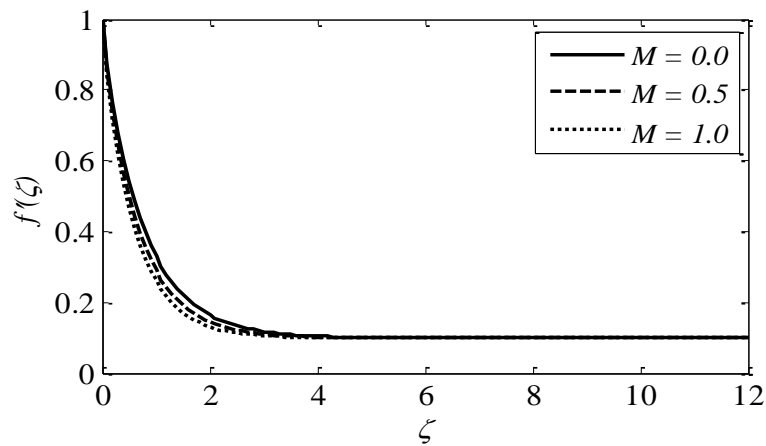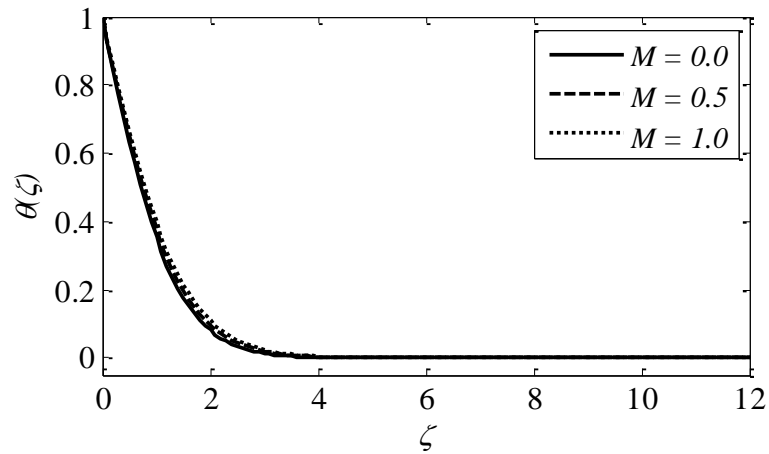

Fig. 6. Profiles of $f'(\zeta)$ for M

Fig. 7. Profiles of $\theta(\zeta)$ for M
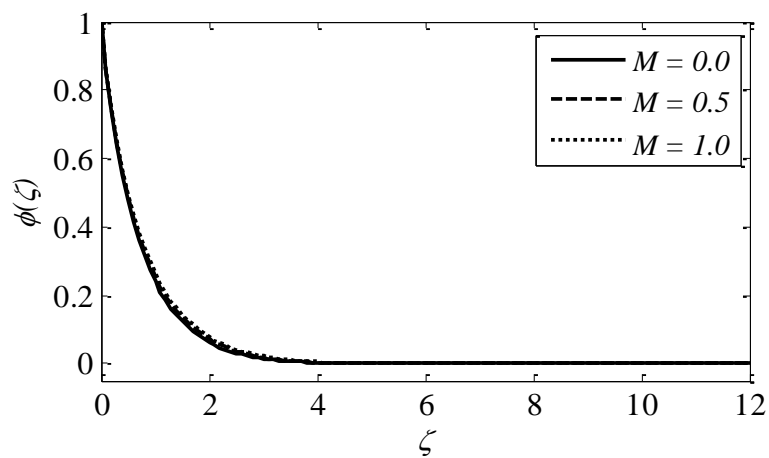
Fig. 8. Profiles of $\phi(\zeta)$ for M

As an elevation in ε, $f(\zeta)$ and boundary layer thickness grow when the free stream velocity is lower than the stretching sheet velocity. $\theta(\zeta)$ and $\phi(\zeta)$ of the surface fall at the surface as ε improves. This is illustrated in Figure 9 to Figure 11.
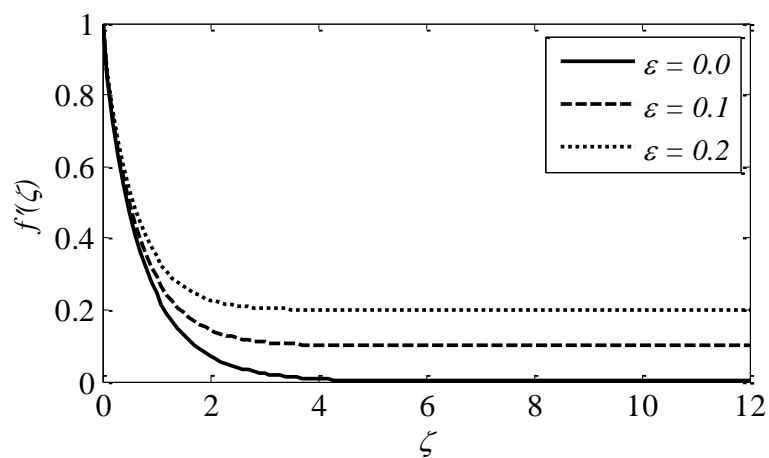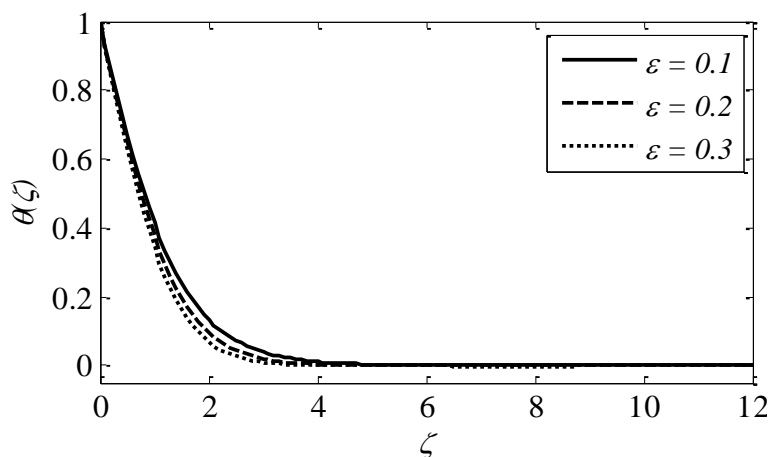

Fig. 9. Profiles of $f'(\zeta)$ for ε

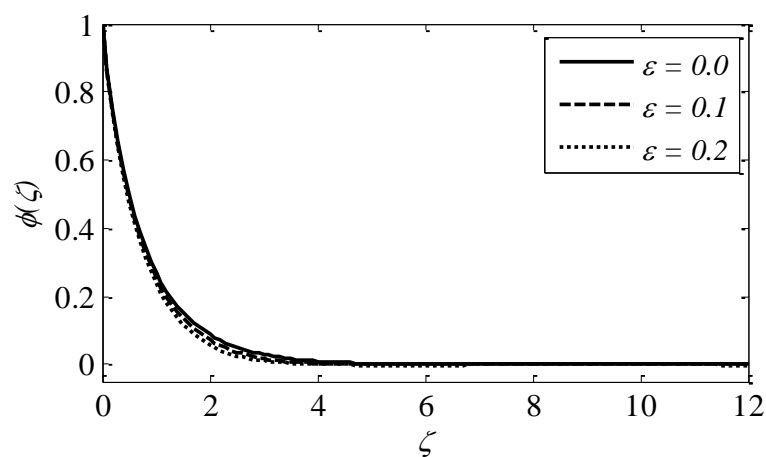**Fig. 10.** Profiles of $\theta(\zeta)$ for ε

Fig. 11. Profiles of $\phi(\zeta)$ for ε

In heat transfer problems, the Prandtl number $\Pr$ is intended to lower the relative thickening of the thermal boundary layer. Since $\Pr$ is a dimensionless number characterized as the proportion of momentum diffusivity to thermal diffusivity, enhancing $\Pr$ values diminish thermal diffusivity. This is given in Figure 12.
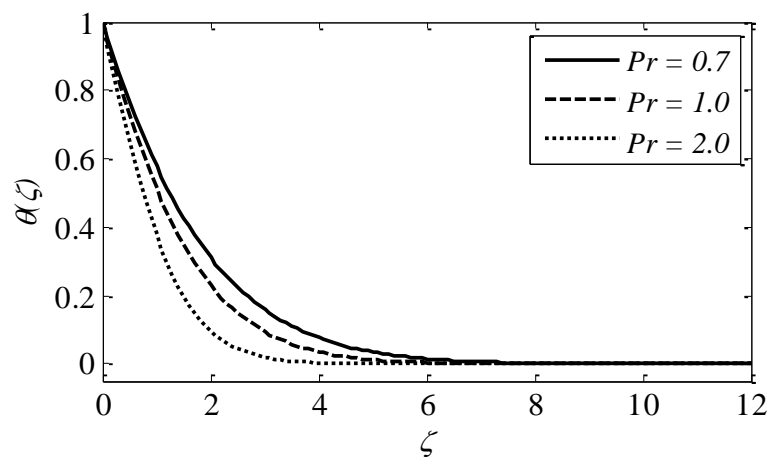

Fig. 12. Profiles of $\theta(\zeta)$ for $\Pr$

When the amount of thermal radiation R is elevated, the fluid acquires more heat, leading in a temperature escalation portrayed in Figure 13.
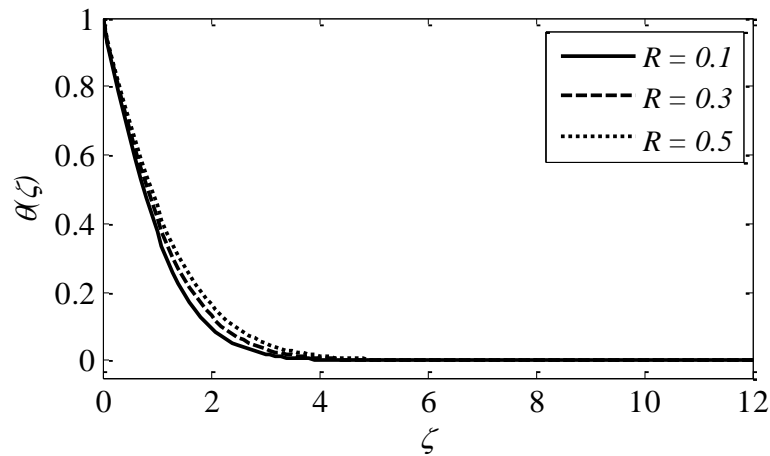
Fig. 13. Profiles of $\theta(\zeta)$ for R

The higher values of parameter Ec have quite an effect on the temperature distribution, rendering this result positive in the perspective that it amplifies the temperature implications given in Figure 14.
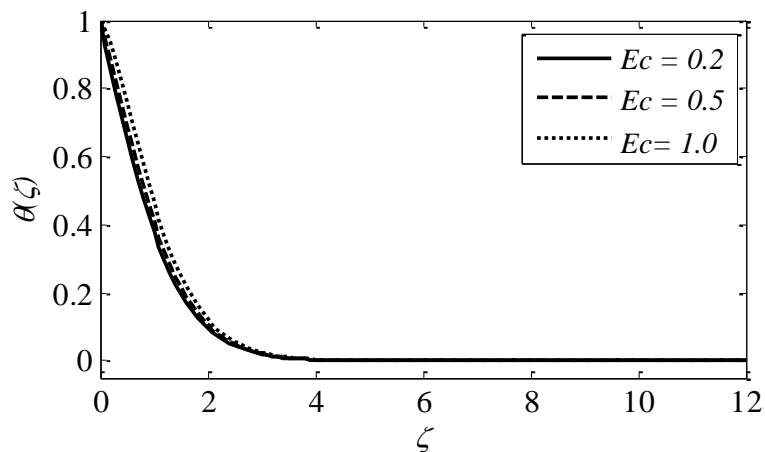
Fig. 14. Profiles of $\theta(\zeta)$ for Ec

The influence of Brownian motion parameter Nb on $\theta(\zeta)$ and $\phi(\zeta)$ is witness in Figure 15 and Figure 17. Brownian motion, in general, helps to heat the fluid in the boundary layer and prevent particle deposition away from the fluid on the surface. As the amount of Nb in the fluid grows, the temperature rises and the concentration drops.
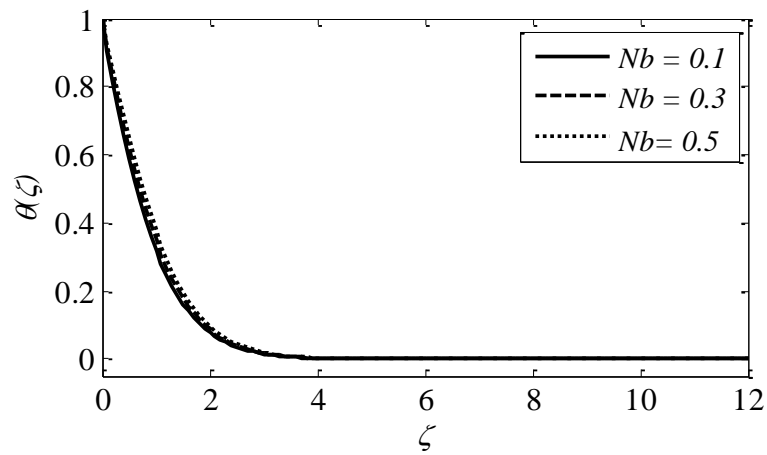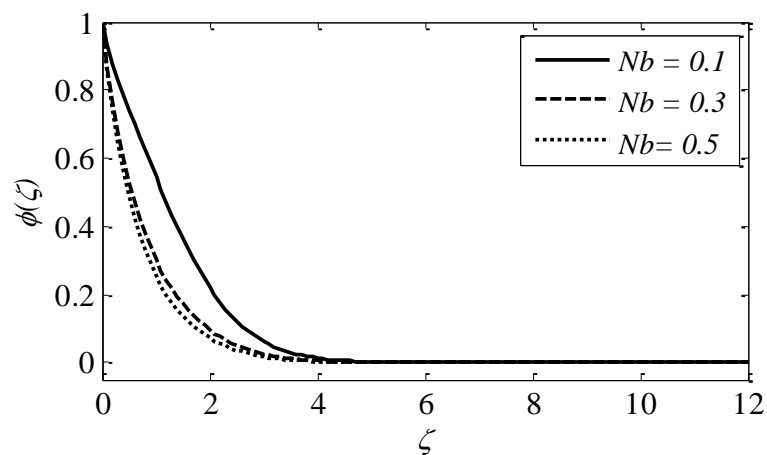
Fig. 15. Profiles of $\theta(\zeta)$ for Nb

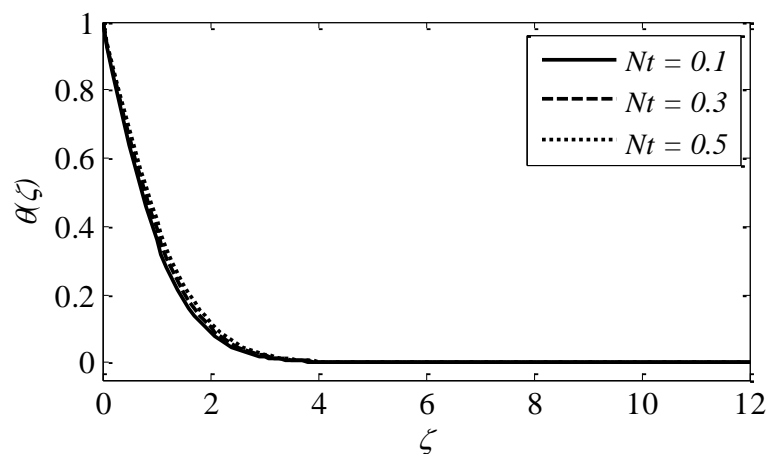**Fig. 16.** Profiles of $\phi(\zeta)$ for Nb

Fig. 17. Profiles of $\theta(\zeta)$ for Nt

The influence of the thermophoresis parameter Nt on $\theta(\zeta)$ and $\phi(\zeta)$ is portrayed in Figure 16 and Figure 18. It is reported that when Nt climbs, so does the temperature and the fraction of nanoparticles. Since both are directly proportional to Nt.
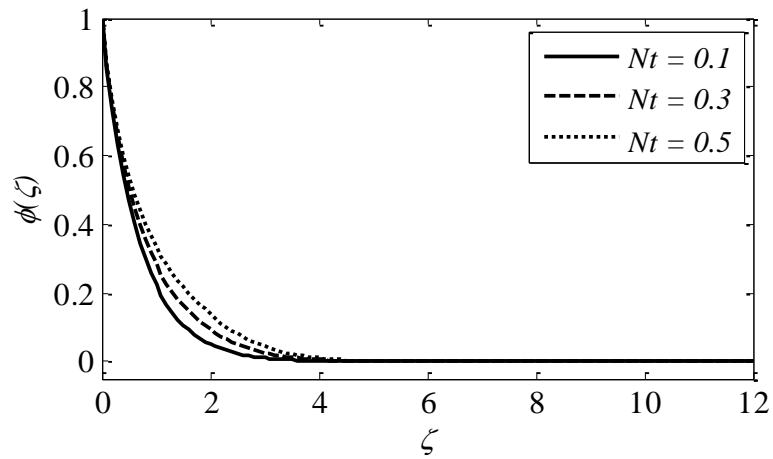
Fig. 18. Profiles of $\phi(\zeta)$ for Nt

Figure 19 illustrates that as the Lewis number Le grows, the $\phi(\zeta)$ of nanoparticles drops. Larger values of Le relate to a poorer Brownian diffusion coefficient, leading in a diminution in the concentration distribution of nanoparticles.

Fig. 19. Profiles of $\phi(\zeta)$ for Le

The consequence of a chemical reaction parameter on $\phi(\zeta)$ is visualized in Figure 20. It has been recognised that as the chemical reaction parameter grows, the concentration lowers.
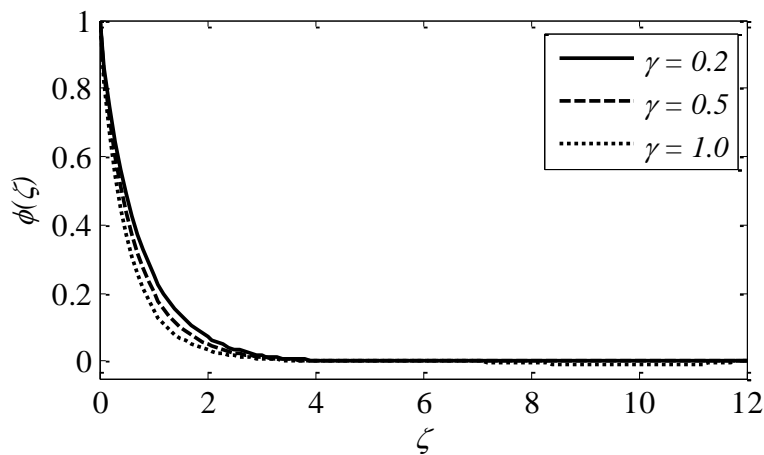
Fig. 20. Profiles of $\phi(\zeta)$ for γ
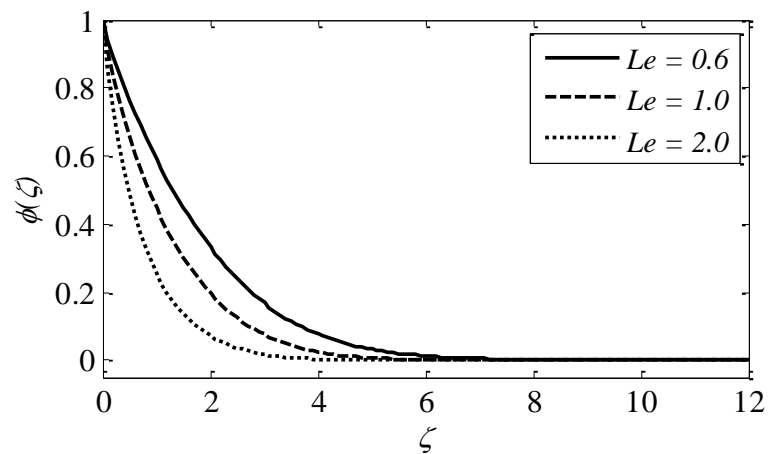
From Figure 21, it is illustrated that skin friction coefficient enhances with λ and drops with M. Figure 22 gives the impact of R and ε on heat transfer rate. This consequence is clearly positive in the sense that a boost in R and ε values lead to a rise in the Nusselt number. Figure 23 illustrates the influence of ε and γ on mass transfer rate. This influence is clearly positive, as higher values of ε and γ lead to higher Sherwood numbers.
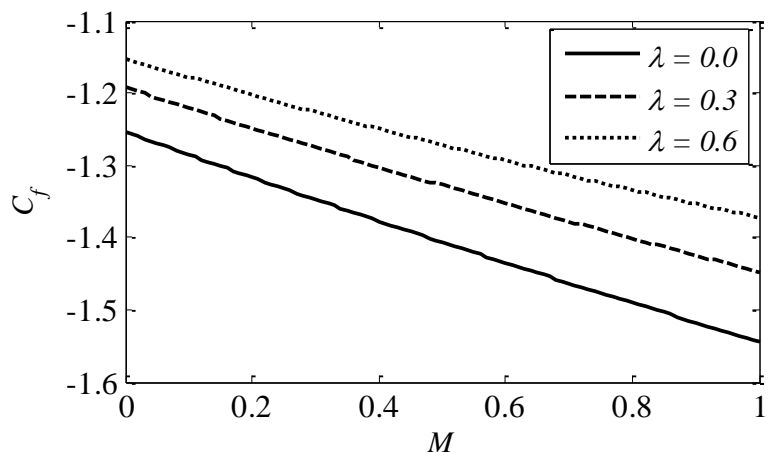
Fig. 21. Profiles of C_f for λ and M
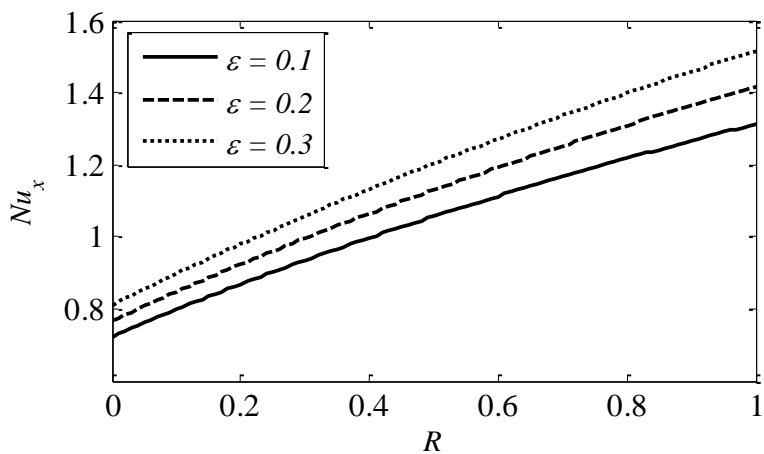
Fig. 22. Profiles of Nu_x for ε and R

Fig. 23. Profiles of Sh_x for ε and γ

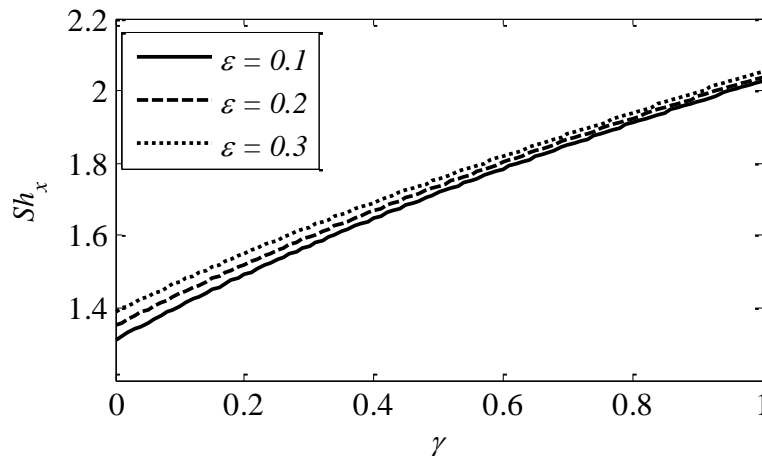A correlation with existing records was executed to properly assess the reliability of our research, and we gained immense agreements, as expressed in Table 2.

Table 2
Comparison of $-\theta'(0)$ for different values of M, Pr, Ec and R in the absence of remaining parameters

Ec	M	R	Pr	Bidin and Nazar [36]	Ishak [37]	Reddy and Shankar [38]	HAM
0.0	0.0	0.0	1.0	0.9547	0.9547	0.9548	0.954783
0.0	0.0	0.0	3.0	1.8691	1.8691	1.8692	1.869067
0.0	0.0	1.0	1.0	0.5315	0.5315	0.5311	0.531503
0.0	1.0	0.0	1.0	0.8611	--	0.8611	0.861427
0.9	0.0	0.0	1.0	--	0.5385	--	0.538541
0.9	0.0	0.0	3.0	--	0.8301	--	0.830137
0.9	0.0	1.0	1.0	--	0.3343	--	0.334521
0.9	0.0	1.0	3.0	--	0.6055	--	0.605519

4. Conclusions

We assessed the MHD stagnation point flow of Williamson fluid over an exponential stretching sheet considering the contribution of various factors in the research work. The noteworthy facts are summed up here.

I. The fluid velocity dropped when λ was elevated, while the Skin friction coefficient rose.
II. When ε is elevated, the velocity profile raises, while the temperature and concentration profiles diminish.
III. The thermal boundary layer thickness lowers as the Prandtl number raises, whereas the radiation parameter has the flip consequence.
IV. Concentration profiles drop as Le and γ are elevated.
V. Nusselt number accelerates with ε and R.

References
[1]   Choi, S. US, and Jeffrey A. Eastman. *Enhancing thermal conductivity of fluids with nanoparticles*. No. ANL/MSD/CP-84938; CONF-951135-29. Argonne National Lab. (ANL), Argonne, IL (United States), 1995.
[2]   Hayat, Tasawar, Rai Sajjad, Ahmed Alsaedi, Taseer Muhammad, and Rahmat Ellahi. "On squeezed flow of couple stress nanofluid between two parallel plates." *Results in Physics* 7 (2017): 553-561. https://doi.org/10.1016/j.rinp.2016.12.038

[3]   Makinde, Oluwole D., and A. Aziz. "Boundary layer flow of a nanofluid past a stretching sheet with a convective boundary condition." *International Journal of Thermal Sciences* 50, no. 7 (2011): 1326-1332. https://doi.org/10.1016/j.ijthermalsci.2011.02.019

[4]   Mahanthesh, B., B. J. Gireesha, and I. L. Animasaun. "Exploration of non-linear thermal radiation and suspended nanoparticles effects on mixed convection boundary layer flow of nanoliquids on a melting vertical surface." *Journal of Nanofluids* 7, no. 5 (2018): 833-843. https://doi.org/10.1166/jon.2018.1521

[5]   Bhatti, M. M., M. Ali Abbas, and M. M. Rashidi. "Analytic study of drug delivery in peristaltically induced motion of non-Newtonian nanofluid." *Journal of Nanofluids* 5, no. 6 (2016): 920-927. https://doi.org/10.1166/jon.2016.1270

[6]   Gul, Taza, Saleem Nasir, Saeed Islam, Zahir Shah, and M. Altaf Khan. "Effective Prandtl Number Model Influences on the γAl2O3-H2O and γAl2O3-C2H6O2 Nanofluids Spray Along a Stretching Cylinder." *Arabian Journal for Science & Engineering (Springer Science & Business Media BV)* 44, no. 2 (2019).

[7]   Ibrahim, S. M., G. Lorenzini, P. Vijaya Kumar, and C. S. K. Raju. "Influence of chemical reaction and heat source on dissipative MHD mixed convection flow of a Casson nanofluid over a nonlinear permeable stretching sheet." *International Journal of Heat and Mass Transfer* 111 (2017): 346-355. https://doi.org/10.1016/j.ijheatmasstransfer.2017.03.097

[8]   Mabood, F., S. M. Ibrahim, P. V. Kumar, and G. Lorenzini. "Effects of slip and radiation on convective MHD Casson nanofluid flow over a stretching sheet influenced by variable viscosity." *Journal of Engineering Thermophysics* 29, no. 2 (2020): 303-315. https://doi.org/10.1134/S1810232820020125

[9]   Kumar, Prathi V., Shaik M. Ibrahim, and Giulio Lorenzini. "The study of three dimensional radiative mhd casson nanofluid over an exponential porous stretching sheet with heat source under convective boundary conditions." *International Journal of Heat and Technology* 36, no. 1 (2018): 1-10. https://doi.org/10.18280/ijht.360101

[10]   Reddy, P. Sudarsana, and P. Sreedevi. "MHD boundary layer heat and mass transfer flow of nanofluid through porous media over inclined plate with chemical reaction." *Multidiscipline Modeling in Materials and Structures* 17, no. 2 (2020): 317-336. https://doi.org/10.1108/MMMS-03-2020-0044

[11]   Kumar, P. Vijaya, S. Mohammed Ibrahim, and G. Lorenzini. "Investigation of the Heat Transfer and Flow Characteristics on Hiemenz Flow under the Influence of Heat Source and Thermal Radiation with Hydrodynamic-Thermal Slips Effects." *Journal of Mechanical Engineering Research and Developments* 44, no. 9 (2021): 369-383.

[12]   Khan, Md Shakhaoath, Ifsana Karim, Md Sirajul Islam, and Mohammad Wahiduzzaman. "MHD boundary layer radiative, heat generating and chemical reacting flow past a wedge moving in a nanofluid." *Nano Convergence* 1, no. 1 (2014): 1-13. https://doi.org/10.1186/s40580-014-0020-8

[13]   Daniel, Yahaya Shagaiya, Zainal Abdul Aziz, Zuhaila Ismail, and Faisal Salah. "Impact of thermal radiation on electrical MHD flow of nanofluid over nonlinear stretching sheet with variable thickness." *Alexandria Engineering Journal* 57, no. 3 (2018): 2187-2197. https://doi.org/10.1016/j.aej.2017.07.007

[14]   Mustafa, M., and Junaid Ahmad Khan. "Model for flow of Casson nanofluid past a non-linearly stretching sheet considering magnetic field effects." *AIP Advances* 5, no. 7 (2015): 077148. https://doi.org/10.1063/1.4927449

[15]   Bhatti, Muhammad Mubashir, M. Ali Abbas, and Mohammad Mehdi Rashidi. "A robust numerical method for solving stagnation point flow over a permeable shrinking sheet under the influence of MHD." *Applied Mathematics and Computation* 316 (2018): 381-389. https://doi.org/10.1016/j.amc.2017.08.032

[16]   Mabood, F., W. A. Khan, and AI Md Ismail. "MHD stagnation point flow and heat transfer impinging on stretching sheet with chemical reaction and transpiration." *Chemical Engineering Journal* 273 (2015): 430-437. https://doi.org/10.1016/j.cej.2015.03.037

[17]   Abbas, Z., M. Sheikh, and I. Pop. "Stagnation-point flow of a hydromagnetic viscous fluid over stretching/shrinking sheet with generalized slip condition in the presence of homogeneous-heterogeneous reactions." *Journal of the Taiwan Institute of Chemical Engineers* 55 (2015): 69-75. https://doi.org/10.1016/j.jtice.2015.04.001

[18]   Malik, M. Y., T. Salahuddin, Arif Hussain, S. Bilal, and M. Awais. "Homogeneous-heterogeneous reactions in Williamson fluid model over a stretching cylinder by using Keller box method." *AIP Advances* 5, no. 10 (2015): 107227. https://doi.org/10.1063/1.4934937

[19]   Zehra, Iffat, Malik Muhammad Yousaf, and Sohail Nadeem. "Numerical solutions of Williamson fluid with pressure dependent viscosity." *Results in Physics* 5 (2015): 20-25. https://doi.org/10.1016/j.rinp.2014.12.002

[20]   Bakar, Fairul Naim Abu, and Siti Khuzaimah Soid. "MHD Stagnation-Point Flow and Heat Transfer Over an Exponentially Stretching/Shrinking Vertical Sheet in a Micropolar Fluid with a Buoyancy Effect." *Journal of Advanced Research in Numerical Heat Transfer* 8, no. 1 (2022): 50-55.

[21]   Mabood, Fazle, Sheikh M. Ibrahim, Giulio Lorenzini, and Enrico Lorenzini. "Radiation effects on Williamson nanofluid flow over a heated surface with magnetohydrodynamics." *International Journal of Heat and Technology* 35, no. 1 (2017): 196-204. https://doi.org/10.18280/ijht.350126

[22]   Ibrahim, S. Mohammed, Prathi Vijaya Kumar, and Oluwole Daniel Makinde. "Chemical reaction and radiation effects on non-Newtonian fluid flow over a stretching sheet with non-uniform thickness and heat source." In *Defect*

and Diffusion Forum, vol. 387, pp. 319-331. Trans Tech Publications Ltd, 2018. https://doi.org/10.4028/www.scientific.net/DDF.387.319

[23] Thirupathi, G., K. Govardhan, and G. Narender. "Radiative Magnetohydrodynamics Casson Nanofluid Flow and Heat and Mass Transfer past on Nonlinear Stretching Surface." *Journal of Advanced Research in Numerical Heat Transfer* 6, no. 1 (2021): 1-21.

[24] Rosaidi, Nor Alifah, Nurul Hidayah Ab Raji, Siti Nur Hidayatul Ashikin Ibrahim, and Mohd Rijal Ilias. "Aligned Magnetohydrodynamics Free Convection Flow of Magnetic Nanofluid over a Moving Vertical Plate with Convective Boundary Condition." *Journal of Advanced Research in Fluid Mechanics and Thermal Sciences* 93, no. 2 (2022): 37-49. https://doi.org/10.37934/arfmts.93.2.3749

[25] Osman, Husna Izzati, Nur Fatihah Mod Omar, Dumitru Vieru, and Zulkhibri Ismail. "A Study of MHD Free Convection Flow Past an Infinite Inclined Plate." *Journal of Advanced Research in Fluid Mechanics and Thermal Sciences* 92, no. 1 (2022): 18-27. https://doi.org/10.37934/arfmts.92.1.1827

[26] Japili, Nirwana, Haliza Rosali, and Norfifah Bachok. "Slip Effect on Stagnation Point Flow and Heat Transfer Over a Shrinking/Stretching Sheet in A Porous Medium with Suction/Injection." *Journal of Advanced Research in Fluid Mechanics and Thermal Sciences* 90, no. 2 (2022): 73-89. https://doi.org/10.37934/arfmts.90.2.7389

[27] Pop, Eric. "Energy dissipation and transport in nanoscale devices." *Nano Research* 3, no. 3 (2010): 147-169. https://doi.org/10.1007/s12274-010-1019-z

[28] Ajayi, T. M., A. J. Omowaye, and Isaac Lare Animasaun. "Viscous dissipation effects on the motion of Casson fluid over an upper horizontal thermally stratified melting surface of a paraboloid of revolution: boundary layer analysis." *Journal of Applied Mathematics* 2017 (2017). https://doi.org/10.1155/2017/1697135

[29] Khan, Ansab Azam, Khairy Zaimi, and Teh Yuan Ying. "Stagnation point flow of Williamson nanofluid towards a permeable stretching/shrinking sheet with a partial slip." *CFD Letters* 12, no. 6 (2020): 39-56. https://doi.org/10.37934/cfdl.12.6.3956

[30] Rajput, Govind R., Bipin P. Jadhav, Vishwambhar S. Patil, and S. N. Salunkhe. "Effects of nonlinear thermal radiation over magnetized stagnation point flow of Williamson fluid in porous media driven by stretching sheet." *Heat Transfer* 50, no. 3 (2021): 2543-2557. https://doi.org/10.1002/htj.21991

[31] Kumar, Prathi Vijaya, S. Mohammed Ibrahim, and Giulio Lorenzini. "Thermal Radiation and Heat Source Effects on MHD Non-Newtonian Fluid Flow over a Slandering Stretching Sheet with Cross-Diffusion." In *Defect and Diffusion Forum*, vol. 388, pp. 28-38. Trans Tech Publications Ltd, 2018. https://doi.org/10.4028/www.scientific.net/DDF.388.28

[32] Hayat, T., S. A. Shehzad, and A. Alsaedi. "Soret and Dufour effects on magnetohydrodynamic (MHD) flow of Casson fluid." *Applied Mathematics and Mechanics* 33, no. 10 (2012): 1301-1312. https://doi.org/10.1007/s10483-012-1623-6

[33] Liao, Shijun. *Beyond Perturbation: Introduction to the Homotopy Analysis Method*. CRC Press, 2011.

[34] Ibrahim, S. M., P. V. Kumar, G. Lorenzini, and E. Lorenzini. "Influence of Joule heating and heat source on radiative MHD flow over a stretching porous sheet with power-law heat flux." *Journal of Engineering Thermophysics* 28, no. 3 (2019): 332-344. https://doi.org/10.1134/S1810232819030044

[35] Hamrelaine, Salim, Fateh Mebarek-Oudina, and Mohamed Rafik Sari. "Analysis of MHD Jeffery Hamel flow with suction/injection by homotopy analysis method." *Journal of Advanced Research in Fluid Mechanics and Thermal Sciences* 58, no. 2 (2019): 173-186.

[36] Bidin, Biliana, and Roslinda Nazar. "Numerical solution of the boundary layer flow over an exponentially stretching sheet with thermal radiation." *European Journal of Scientific Research* 33, no. 4 (2009): 710-717.

[37] Ishak, Anuar. "MHD boundary layer flow due to an exponentially stretching sheet with radiation effect." *Sains Malaysiana* 40, no. 4 (2011): 391-395.

[38] Reddy, Ch. Achi, and B. Shankar. "MHD stagnation point flow in a boundary layer flow of a nanofluid over a stretching sheet in the presence of viscous dissipation and chemical reaction." *Mechanics, Material Science & Engineering* 4 (2017): 45-57. https://doi.org/10.1016/j.matpr.2017.07.080